Please refer to section 3 and 4 of the Author Guidelines for full details regarding formatting

Page formatting
Font size: 10 pt (except for title, synopsis and authors' biographies)
Page size: A4 (21cm x 29.7cm)
Margin (right and left): 2.5cm
Text: Justified and singled spaced, using indent to signify new paragraph
Columns: One

Torque control for diesel mechanical and hybrid propulsion on naval vessels

Title of paper
Purpose: Clearly indicates the subject of the paper
Font size: 12 pt bold; left-aligned

R D Geertsma, MSc, CEng, MIMarEST[a&b], Dr. R R Negenborn[a], Ir. K Visser, FIMarEST

[a]*Delft University of Technology, The Netherlands;* [b]*Netherlands Defence Academy, The Ne*
*Corresponding author. Email: r.d.geertsma@tudelft.nl

Authors
Include: full names, honours, academic qualifications and affiliations
Corresponding author's email for enquiries
Font size: 10 pt; affiliations in italics; left-aligned

Synopsis

strict requirements regarding reduction of fuel consumption, for en-
es are at ractive for naval propulsion due to their low fuel consump-
gies they suffer from overloading and can only provide limited
control an trol regimes. In
simulation experiments, we investigate the resulting prop f several dy-
namical models of ship components allows investigating p al loading,
fuel consumption, acceleration and cavitation noise emis e loading
with 4% and torque control combined with advanced pitch formance,
while further reducing thermal loading, fuel consumption a hat uses the
proposed strategies will make diesel engines even more attracti pulsion.

Synopsis
Purpose: Concise summary of the paper
Font size: 9 pt including 'Synopsis' title
Title: 'Synopsis' title should be centred
Word count: 500 maximum
Indented: Right and left by 1cm

Keywords: Mechanical propulsion; Non-linear control systems; Marine systems

Keywords
Purpose: Enable accurate searching
Number: 5-6 keywords or phrases
Punctuation: Semi-colons

1 Introduction

Nowadays, all navies have t ce environmental impact and improve endurance, thus reducing their dependency ich are highly fuel efficient, are often the preferred power source for naval ships. Due t and low power density of diesel engine driven ships, gas turbin s are, however, often still the preferred engine type for providing boost power on naval combatants. On the other hand, top speed, such as patrol vessels (Lyster and Dawe, 2015) and the Royal Danish Navy ships, typically use diesel engines for their main propulsion. Furthermore, many eed propulsion and some navies even use multiple diesel engines per shaft for to *eldt* class air defence frigates. Finally, direct drive diesel engines can be used in s in the *Holland class* patrol vessel (Blokland and van Dijk, 2015).

Introduction
Purpose: To convey the reasons for writing the paper

The main challenge to apply diesel engines on naval vessels is to prevent overloading, particularly during acceleration manoeuvres and in heavy weather conditions. Diesel engines have shown to be susceptible to overloading when applied as direct drive propulsion for frigates in the Royal Netherlands Navy (RNLN) and Canadian Navy (van Spronsen and Toussain, 2001; Guillemette and Bussières, 1997). This overloading occurs when engine torque exceeds the overloading criterion of the operating envelope, which, at reduced engine speeds, is limited due to the turbocharger limit (Klein Woud and Stapersma, 2012). Furthermore, dynamic overloading occurs when the air acces ratio becomes too low, so insufficient air is available in the cylinder during the combustion process (Stapersma, 2010).

Overloading in heavy weather is caused by two effects: The added resistance, due to waves and wind, causes a torque increase for a given engine speed, and orbital velocity fluctuations in waves cause fluctuating wake speed (Gerritsma and Beukelman, 1972; Gerritsma, 1989; Taylor, 1933). These wake speed variations in the propeller cause fluctuation of shaft speed and torque. With conventional speed control this leads to fluctuating engine speed and fuel rack, which is proportional to case of dynamic overloading due to waves as measured on RNLN M-frigates ilarly, overloading can be caused by acceleration and sharp turns, particularly

Biographical notes
Purpose: To give brief biographical summary for each author
Word count: 50 words approximately per author
Font size: 8 pt, Author names in bold

Authors' Biographies

Lt Cdr Rinze Geertsma currently ology and the Netherlands Defence Academy on control strategies for hybrid ship systems in a flexibl ssion context. He has previously been in charge of the Marine Engineering Department of *HNLMS de Ruyter* and *HNLMS Tromp*. Earlier exper nce includes sea appointments, system and project engineering and in service support for the fleet.

Dr. Rudy Negenborn is associate professor in automatic control & coordination of transport technology at the Section Transport Engineering & Logistics of Department Maritime & Transport Technology, Delft University of Technology. Dr. Negenborn's research interests include multi-agent systems, distributed control, model predictive control for applications in (waterborne) networked transport systems.

Ir. Klaas Visser (RAdm (ME) ret) is assistant professor in Marine Engineering at the Section Ship Design, Production and Operations of the Department Maritime & Transport Technology, Delft University of Technology. His research interests include Maritime Systems Integration, especially Hybrid Propulsion Systems and innovative hybrid maritime power production and energy storage systems.

Prof. ir. Hans Hopman is professor of ship design and chairman of the Department Maritime & Transport Technology, Delft University of Technology.

Figures
Purpose: To convey the essence of the paper to the reader
Layout: Two figures side by side, or one figure across page

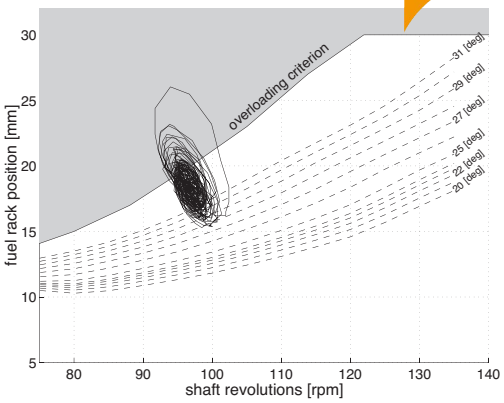

Figure 1: Dynamic overloading due to waves plotted in the phase plane, as measured on RNLN M-frigates ©IFAC 2001 (van Spronsen and Toussain, 2001).

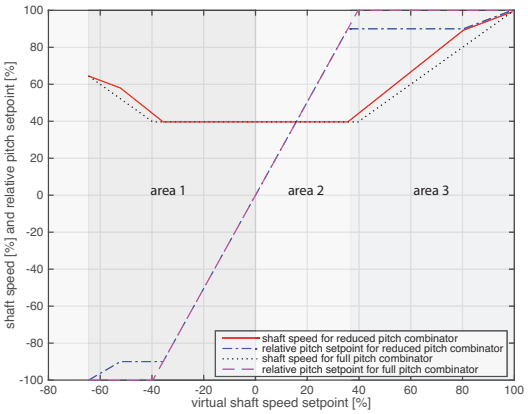

Figure 2: Two typical combinator curves for diesel mechanical propulsion with reduced and full pitch in speed control area.

Trademarks
Purpose: To acknowledge a proprietary term or trade mark
© / ® / ™

l combinator curve and speed control of the diesel engine. The fixed combinator cur the setting from the lever and the propeller pitch and engine speed references. Th of three areas, as shown in Figure 2. In area 1, reversing propeller pitch achi g or stopping. In this paper, we will focus on positive speed settings, because the ship rea 2, engine speed is kept constant at minimum engine speed. In this *pitch control regime*, thrust can only be controlled by changing propeller pitch, because the engine cannot run at speeds below minimum. Furthermore, the engine load is well below its limitations. Therefore, we propose to leave the control strategy in this area unchanged. In area 3, thrust is primarily controlled by changing engine speed. In this *speed control regime*, pitch reduction is currently used to prevent engine overloading, but pitch could also be used to improve other performance attributes, such as fuel consumption, engine thermal loading, manoeuvrability and cavitation noise.

While many authors have suggested speed control leads to unnecessary engine load disturbance, even most proposed advanced control strategies still use speed control. For example, Guillemette and Bussières (1997) propose adaptive speed control by modifying the amplification of the speed feedback signal real-time and Xiros (2002) proposes H_∞ state feedback controller synthesis with a control objective to reduce shaft speed fluctuation. Both these control methods can improve engine load disturbance rejection, but primarily use engine speed feedback.

Even though actively changing propeller pitch during waves can improve disturbance rejection and engine overloading, this would require a high amount of pitch actuation (van Spronsen and Toussain, 2001; Vrijdag, 2009). Continuous pitch actuation might increase wear on the propeller actuation mechanism, although Godjevac (2009) found that wear mechanisms do not preclude development of faster Controllable Pitch Propellers (CPP). Nevertheless, reducing loading fluctuation without continuously actuating pitch would be preferred, as fast pitch actuation systems are not available yet and are likely to increase required maintenance.

Therefore, this paper first proposes torque control for diesel engines as an alternative to speed control, aiming to reduce the effect of dynamic overloading of engines without continuous pitch actuation. Furthermore, the paper will investigate how adaptively changing pitch in combination with torque control can also improve other performance parameters, such as fuel consumption, acceleration and noise emission. The paper is organised as follows. In Section 2, the mechanical propulsion system of a patrol vessel is described and the dynamical model is introduced. In Section 3, we describe traditional speed control, propose an alternative *torque control* strategy and propose schedules to investigate the influence of varying pitch. In Section 4, we present the outcomes of simulation experiments to assess the static performance at varying speed and during acceleration manoeuvres under various dynamic conditions. Finally, in Section5, conclusions and further research are summarised.

2 System description

For a naval vessel, the mechanical propulsion system with diesel engines as prime movers typically consists of two shaftlines for redundancy. In this paper, we consider a mechanical propulsion system with one diesel engine

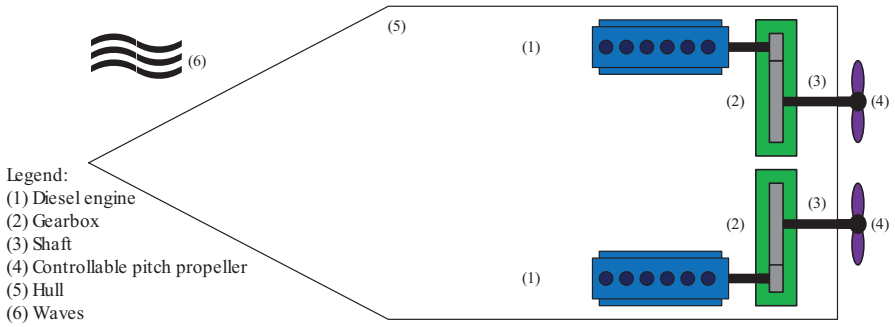

Figure 3: Typical mechanical propulsion system layout for a naval vessel.

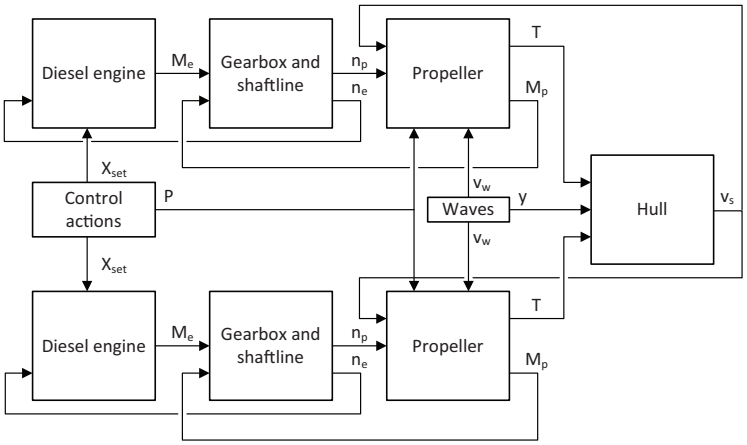

Figure 4: Schematic presentation of direct drive propulsion system for naval vessel showing coupling between models.

per shaft. The mechanical propulsion plant consists of two diesel engines, gearboxes, shafts and controllable pitch propellers (CPP) and is used to propel the ship, as illustrated in Figure 3. Furthermore, the influence of waves acts as a disturbance on the ship system. Figure 4 presents the model representation of this system, showing how the system components are coupled. Below, the details of the models are described.

2.1 Diesel engine model

Many different models with varying complexity are available for diesel engines, ranging from mathematical models that predict fuel consumption and include a first order equation of motion (Shi et al., 2010), via complex high order mean value first principle models that include air and exhaust gas flow dynamics (Schulten, 2005; Grimmelius and Stapersma, 2001), to even more complex crank angle models (Kyrtatos and Koumbarelis, 1991). The performance indicators thermal loading, fuel consumption, manoeuvrability and cavitation noise are mainly influenced by the inertia of the mechanical drive and the turbocharger dynamics. Therefore, this research uses a second order average value first principle model for the diesel engine.

The used diesel engine model consists of the following sub-models (Miedema and Lu, 2002):

- The fuel pump model represents the amount of fuel injected per cylinder per engine cycle m_f in g, as a function of the fuel pump setpoint $X_{set}(t)$ in %. It is assumed that fuel injection has a linear relationship with fuel pump setpoint, which is typical for both mechanical fuel pumps and electronic fuel injection systems with common rail fuel injection. The model consists of a first order time delay τ_X in s to represent the inertia of the fuel injection system and the ignition delay and is mathematically described as:

$$\frac{dm_f(t)}{dt} = \frac{C_X X_{set}(t) - m_f(t)}{\tau_X}, \tag{1}$$

where C_X is a constant representing the ratio betw nominal fuel injection and nominal fuel pump setpoint in g.

Equations
Purpose: Demonstrate relationship between factors
Format: All equations must be embedded
Layout: Presented consecutively and be numbered

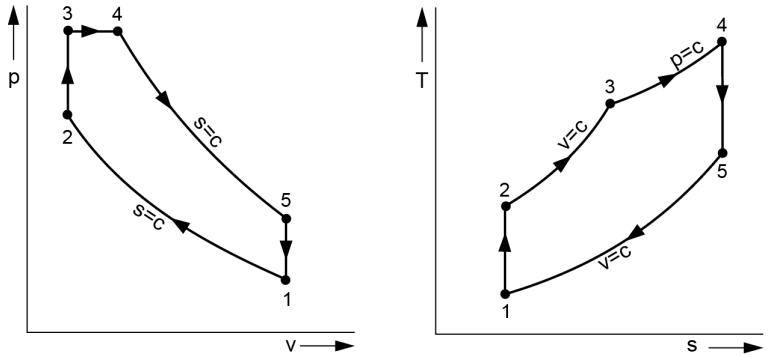

Figure 5: Typical five point Seiliger or dual cycle consisting of compression (1-2), isochoric combustion (2-3), isobaric combustion (3-4) and expansion (4-5) (Klein Woud and Stapersma, 2012).

- The heat release model represents the heat release, which depends on the cylinder inlet pressure p_1 in bar, the amount of injected fuel m_f in g and the engine speed n_e in rev/s. For this model, a constant heat release efficiency η_q based on nominal engine data is assumed and combustion efficiency η_{comb} is considered a function of the air excess ratio λ, according to Betz and Woschni (1986). The released heat is split between a constant volume segment q_{cv} in kJ/kg and a constant pressure segment q_{cp} in kJ/kg in the five point Seiliger proces, according to Miedema and Lu (2002), where the constant volume portion X_{cv} is considered to increase linearly with engine speed at rate $X_{cv,grad}$. The heat release model is summarised as follows:

$$q_{cv}(t) = f_1(m_f(t), n_e(t), p_1(t)) \tag{2}$$
$$q_{cp}(t) = f_2(m_f(t), n_e(t), p_1(t)). \tag{3}$$

- The five point Seiliger process represents the four stages of the diesel engine compression, isochoric and isobaric combustion and expansion process and determines the work produced during these stages. The heat release model determines the heat release during the constant volume and constant pressure segment of the Seiliger proces. The cylinder inlet pressure p_1 in Pa and temperature T_1 in K, the latter of which is assumed constant, are the inputs to the start of the five point Seiliger proces, which is illustrated in Figure 5. The Seiliger cycle equations are presented in Table 1 (Klein Woud and Stapersma, 2012), where V_i, p_i and T_i are the volume in m^3, pressure in Pa and temperature in K at state i, r_c is the effective compression ratio, κ_a is the isentropic index of air, R_a is the gas constant of air in J/kgK, a and b are the Seiliger parameters as determined using Miedema and Lu (2002), $c_{v,a}$ and $c_{p,a}$ are the specific heats at constant volume and pressure for air in J/kgK and n_{exp} is the polytropic exponent for expansion. Moreover, a mechanical loss is deducted from the indicated work, which is assumed to be linear with engine speed and can be expressed in mechanical efficiency η_m. The Seiliger process can be summarised with the following two equations:

$$M_e(t) = f_3(n_e(t), p_1(t), q_{cv}(t), q_{cp}(t)) \tag{4}$$
$$q_{exh}(t) = f_4(n_e(t), p_1(t), q_{cv}(t), q_{cp}(t)), \tag{5}$$

  where M_e is engine torque in kNm and q_{exh} is the specific heat output in kJ/kg from the exhaust gasses, which is used for the exhaust and turbocharger model.

- The exhaust and turbocharger system model estimates the cylinder inlet pressure p_1 in Pa from the specific heat output of the exhaust gasses in kJ/kg (Miedema and Lu, 2002). Furthermore, a time delay τ_{TC} in s is used to model turbocharger inertia, as follows:

$$\frac{dp_1}{dt} = \frac{f_8(q_{exh}) - p_1}{\tau_{TC}}. \tag{6}$$

Tables
Purpose: To present detailed data
Layout: Two tables side by side, or one table across page. Exceptional amounts of data can be presented in landscape

Table 1: Seiliger cycle equations

Seiliger stage	**Volume** V	**Pressure** p	**Temperature** T	**Specific work** w	**Heat** q
Compression 1-2	$\frac{V_1}{V_2} = r_c$	$\frac{p_2}{p_1} = r_c^{\kappa_a}$	$\frac{T_2}{T_1} = r_c^{(\kappa_a - 1)}$	$w_{12} = \frac{R_a(T_2 - T_1)}{n_c - 1}$	–
Isochoric combustion 2-3	$\frac{V_3}{V_2} = 1$	$\frac{p_3}{p_2} = a$	$\frac{T_3}{T_2} = a$	–	$q_{23} = c_{v,a}(T_3 - T_2)$
Isobaric combustion 3-4	$\frac{V_4}{V_3} = b$	$\frac{p_4}{p_3} = 1$	$\frac{T_4}{T_3} = b$	$w_{34} = R_a(T_4 - T_3)$	$q_{34} = c_{p,a}(T_4 - T_3)$
Expansion 4-5	$\frac{V_5}{V_4} = \frac{r_c}{b}$	$\frac{p_4}{p_5} = (\frac{r_c}{b})^{n_e}$	$\frac{T_4}{T_5} = (\frac{r_c}{b})^{n_e - 1}$	$w_{45} = \frac{R_a(T_5 - T_4)}{n_e - 1}$	–

In summary, after substituting (2) and (3) in (4) and (5) in (6), the diesel engine model consists of a system of differential-algebraic equations (DAE's), as follows:

$$\frac{dm_f(t)}{dt} = \frac{C_X X_{set}(t) - m_f(t)}{\tau_X} \tag{7}$$

$$\frac{dp_1(t)}{dt} = \frac{f_{10}(n_e(t), p_1(t), m_f(t))}{\tau_{TC}} \tag{8}$$

$$M_e(t) = f_{11}(m_f(t), n_e(t), p_1(t)). \tag{9}$$

2.2 Gearbox model and shaft line model

The gearbox and shaft line model predicts the losses in the gearbox and accounts for the speed reduction of the gearbox. Furthermore, this model represents the equation of motion for all shafts connected to the gearbox and accounts for all inertia influencing the rotation of the shaft. This is the inertia of the engine, shaft line, gearbox, propeller and entrained water. Gearbox loss prediction is very complex, but can be simplified with a linear gearbox loss function (Godjevac et al., 2015). This function has been shown to give good resemblance with more complex heat loss models and can be fitted well to manufacturer data (de Waard, 2014, 2015). Mathematically the gearbox losses and equation of motion can be described as follows:

$$\frac{dn_p(t)}{dt} = \frac{dn_e(t)}{idt} = \frac{i(M_e(t) - M_{gb}(t)) - M_p(t)}{I_{tot} 2\pi} \tag{10}$$

$$M_{gb}(t) = a_{gb} + b_{gb} n_e(t) + c_{gb} M_e(t), \tag{11}$$

where n_p is propeller and shaft rotational speed in rev/s, i is the gearbox reduction ratio, M_{gb} is the torque loss in the gearbox in kNm, M_p is the propeller torque in kNm, I_{tot} is the total moment of inertia in kgm^2 and the parameters a_{gb}, b_{gb} and c_{gb} are the gearbox loss function parameters as defined according to de Waard (2014). Combined these equations can be classified as a system of DAE's.

2.3 Propeller model

Various propeller models and data series are available, such as the Taylor, and Gawn Series (Taylor, 1933; Gawn, 1952). The most widely used propeller data series are the Wageningen B and Ka-series (Kuiper, 1992). However, all these series consist of open water diagrams for fixed pitch propeller designs. Recently, the Maritime Research Institute Netherlands (MARIN) has developed a new methodology to measure and evaluate the two quadrant open water diagram of CPP's and used this methodology to develop the Wageningen C- and D-series for open and ducted CPP's. The propellers in these series represent 'contemporary and practical CPP designs' (Dang et al., 2012). We use the Wageningen C4-40 propeller because this propeller is representative for the behaviour of propellers in general and

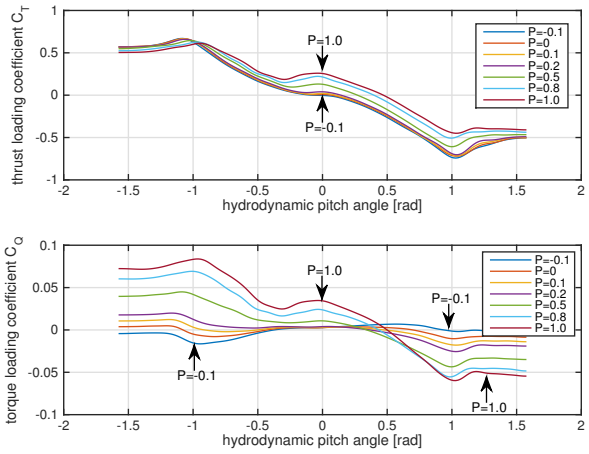

Figure 6: Two quadrant open water diagram of Wageningen C4-40 propeller for various pitches.

adequate for this purpose. Moreover, the C4-40 propeller open water diagram is publicly available, as shown in Figure 6 (Dang et al., 2013).

The propeller model represents the propeller torque Q in kNm and thrust T in kN as a function of shaft speed n_p in rev/s, ship speed v_s in kts, propeller pitch ratio P and wakefield disturbance due to waves v_w in m/s. The disturbed advance speed of the water relative to the propeller v_{a_d} in m/s and the hydrodynamic pitch angle β in rad are expressed as follows:

$$v_{a_d}(t) = v_s(t)(1-w) + v_w(t) \tag{12}$$

$$\beta(t) = arctan\left(\frac{v_{a_d}(t)}{0.7\pi n_p(t)D}\right), \tag{13}$$

where w is the wake fraction, which is considered constant and D is the propeller diameter in m.

With the hydrodynamic pitch angle β in rad and the propeller pitch ratio P, the thrust and torque loading coefficients C_T and C_Q can be obtained from the open water diagram data from Dang et al. (2013), using linear interpolation. Subsequently, the open water torque Q in kNm and thrust T in kN are represented by the following equations:

$$v_r(t) = \sqrt{v_{a_d}(t)^2 + (0.7\pi n_p(t)D)^2} \tag{14}$$

$$T(t) = C_T(t)\frac{1}{2}\rho v_r(t)^2\frac{\pi}{4}D^2 \tag{15}$$

$$Q(t) = C_Q(t)\frac{1}{2}\rho v_r(t)^2\frac{\pi}{4}D^3. \tag{16}$$

In order to obtain the actual propeller torque M_P in kNm, the relative rotative efficiency of the propeller η_R, which is assumed constant, needs to be accounted for (Klein Woud and Stapersma, 2012):

$$M_P(t) = \frac{Q(t)}{\eta_R}. \tag{17}$$

In summary, the propeller can be represented by the following system of algebraic equations (AE's):

$$T(t) = f_{13}(v_s(t), v_w(t), n_p(t), P(t)) \tag{18}$$

$$M_p(t) = f_{14}(v_s(t), v_w(t), n_p(t), P(t)). \tag{19}$$

2.4 Hull model

The hull model can be mathematically described as follows:

$$\frac{dv_s(t)}{dt} = \frac{\left(k_p T(t) - \frac{R(v_s(t))}{1-t}\right)}{m}, \tag{20}$$

where k_p is the number of propellers and R is the ship resistance in kN, which is considered a function of ship speed v_s in m/s, t is the thrust deduction factor, which is assumed constant and m is the ships mass in kg. The resistance is represented by a function of ship speed with the following equation (Klein Woud and Stapersma, 2012):

$$R(v_s) = yc_0 v_s(t)^2, \tag{21}$$

where y is a multiplication factor that can account for additions to the nominal resistance due to fouling of the hull and operational conditions and c_0 is the nominal resistance factor in kg/m, which in the case study is assumed to be constant as the Froude number remains low (Klein Woud and Stapersma, 2012). Although this method simplifies the added resistance due to wind and sea state significantly compared to more accurate methods as proposed in Gerritsma and Beukelman (1972) and more recently in Liu and Papanikolaou (2016), it allows investigating the effect of fouling and operational conditions on the system behaviour very efficiently. In summary the hull can be represented by the following DAE:

$$\frac{dv_s(t)}{dt} = f_{14}(T(t), v_s(t)). \tag{22}$$

2.5 Wave model

In the wave model, two effects represent the influence of waves on the propulsion system. First, an increase in the resistance multiplication factor y accounts for the average added resistance due to waves. Although the actual resistance fluctuates, it is sufficient to represent this fluctuation with an average increase, because the mass of the ship dampens the effect this has on the propulsion plant. Moreover, the disturbance on the wake speed of the water flowing into the propeller due to the orbital movement of the water has much more effect on the propulsion plant dynamics. Secondly, the wakefield disturbance due to waves v_w represents the previously mentioned orbital movement. Even though actual waves show an irregular stochastic spectrum (Aalbers and van Gent, 1984), we consider modelling a single characteristic wave amplitude and frequency (Gerritsma, 1989), sufficient to demonstrate the effect of waves. Including the impact of a realistic spectrum (Taylor, 1933; Gerritsma and Beukelman, 1972) is further work. We consider head waves, meaning the ship sails in opposite direction to the waves. Thus, the wake field disturbance due to waves is expressed as follows (Gerritsma, 1989):

$$v_w(t) = \zeta \omega e^{kz} sin((-kv_{max} - \omega)t) \tag{23}$$

$$k = \frac{\omega^2}{g}, \tag{24}$$

where ζ is the wave amplitude in m, ω is the wave radial frequency in rad/s, k is the wave number, z is the water depth in m at the propeller center, g is the standard gravity in m/s^2 and v_{max} is the ship speed in m/s, which is considered constant, because the influence of ship speed on the frequency is limited.

3 Control strategies

Current traditional and advanced control strategies all use speed control, as argued in the introduction1. After determining the control strategy and constraints for conventional speed control and proposing two combinator curves, a *torque control* strategy is proposed in this section and its constraints are determined. Subsequently, a pitch schedule is proposed to investigate the potential effect of alternative pitch control in combination with torque control.

3.1 Speed control

When diesel engines were first applied for propulsion on naval vessels, preventing thermal overloading of the engine turned out to be challenging (van Spronsen and Toussain, 2001; Guillemette and Bussières, 1997). Initially, severe pitch reduction regimes prevented engine overloading. Vrijdag (2009) reports measurements showing this drastic pitch reduction regime, which causes a reduction in ship speed at the start of acceleration manoeuvres. As an alternative to this regime, Vrijdag (2009) proposes a limitation on the engine acceleration rate, on top of an *angle of attack* control strategy. Thus, the combinator curve and maximum allowed shaft acceleration rate have to be set properly to prevent overloading without pitch reduction.

The schematic representation of speed control is given in Figure 7. The control system can be described as follows:

$$X_{set}(t) = K_P \left(\frac{n_{ref}(t)}{100} - \frac{n_e(t)}{n_{e_{nom}}} \right) + K_I \int_0^t \left(\frac{n_{ref}(t)}{100} - \frac{n_e(t)}{n_{e_{nom}}} \right) dt, \tag{25}$$

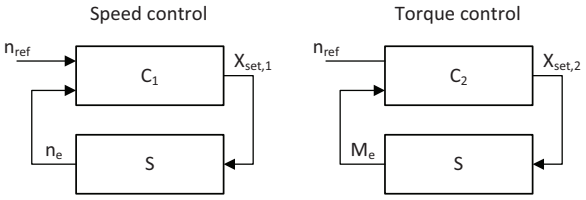

Figure 7: Control loop for mechanical propulsion for speed control and torque control.

Table 2: Speed and torque control parameters

	speed control	**torque control**
proportional gain K_P	2	2
reset rate K_I	0.5	0.5
engine acceleration rate dn_{max}	11 rev/s	
torque increase rate dT_{max}		0.8 kNm/s

where K_P is the proportional gain, K_I is the reset rate, n_{ref} is the reference speed in % and $n_{e_{nom}}$ is the nominal engine speed in rev/s. A typical acceleration time of 60 s from 0% to 100% is given in engine manufacturers documentation. The resulting speed control parameters are listed in Table 2. Furthermore, two combinator curves are proposed: one curve with 10% pitch reduction across the speed control regime and one curve with full pitch across the speed control regime. Both combinator curves are presented in Figure 2.

3.2 Torque control

The objective for the torque control strategy is to reduce engine overloading and fluctuation of torque and thermal loading due to sea state and acceleration manoeuvres (Faber, 1993; Stapersma et al., 2004; Stapersma and Grimmelius, 2009). The idea is that the propulsion plant is self-regulating and torque control eliminates torque and thermal loading fluctuation. This should lead to better operating conditions for the engine. A schematic presentation of torque control is presented in Figure 7. The control system can be described as follows:

$$X_{set}(t) = K_P \left(\left(\frac{n_{ref}(t)}{100} \right)^2 - \frac{M_e(t)}{M_{e_{nom}}} \right) + K_I \int_0^t \left(\left(\frac{n_{ref}(t)}{100} \right)^2 - \frac{M_e(t)}{M_{e_{nom}}} \right) dt, \tag{26}$$

where $M_{e_{nom}}$ is the nominal engine torque in kNm.

In order to maintain the nearly linear relationship between the lever setting and resulting ship speed, a quadratic relationship is taken between lever setting and torque setpoint. As with speed control, the rate of increase of torque has to be limited, first to prevent crossing the temporary operation limit or overloading criterion, secondly to prevent thermal overloading. The resulting torque control parameters are listed in Table 2.

3.3 Adaptive pitch control

With traditional combinator curves, high pitch during acceleration limits the possibility to increase engine speed quickly. This slow engine speed increase in combination with the turbocharger lag causes high thermal loading of the engine. We propose an alternative, schedule-based, pitch control strategy that, first, slowly reduces propeller pitch during acceleration to maintain thrust, then maintains the reduced pitch, and, finally, slowly increases pitch, until reaching the final setpoint. This schedule-based control strategy will be helpful in assessing the potential of pitch optimisation and can be represented mathematically as follows:

$$t \in [t_0, t_0 + 20] : P(t) = 0.9 - 0.01t \tag{27}$$

$$t \in [t_0 + 20, t_0 + 30] : P(t) = 0.7 \tag{28}$$

$$t \in [t_0 + 30, t_0 + 60] : P(t) = 0.7 + 0.01t, \tag{29}$$

where t_0 is the start time of the acceleration manoeuvre in s.

Table 3: Patrol vessel case study model parameters

Hull		**Diesel engine**	
ship mass m	3800e^3 kg	nominal power P_{nom}	5000 kW
number of propellers k_p	2	nominal speed n_{nom}	16.7 rev/s
thrust deduction factor t	0.19	number of cylinders i_e	12
maximum ship speed v_{max}	20 kts	fuel injection constant C_X	2.7 g
design resistance $R_{v_{max}}$	620 kN	fuel pump time delay τ_X	0.02 s
nominal resistance factor c_0	5860 kg/m	heat release efficiency η_q	0.74
Propeller		effective compression ratio r_c	13.8
wake fraction w	0.09	cylinder volume at state 1 V_1	0.0208 m^3
diameter D	3.25 m	nominal pressure at state 1 $p_{1_{nom}}$	4.1e^5 Pa
design pitch P_d	1	temperature at state 1 T_1	313 K
nominal pitch P_{nom}	1	gas constant of air R_a	287 J/kgK
relative rotative efficiency η_R	1	specific heat at constant volume of air $c_{v,a}$	717.5 J/kgK
Gearbox and shaftline		specific heat at constat pressure of air $c_{p,a}$	1004.5 J/kgK
reduction ratio i	4.348	isentropic index of air κ_a	1.4
total moment of inertia I_{tot}	5000 kgm^2	polytropic exponent for expansion n_{exp}	1.353
shaft efficiency η_s	0.99	nominal mechanical efficiency $\eta_{m_{nom}}$	0.95
gearbox loss function parameter a a_{gb}	0.028 kNm	nominal constant volume portion $X_{cv,nom}$	-0.28
gearbox loss function parameter b b_{gb}	0.0453 kNms	constant volume portion gradient $X_{cv,grad}$	-1
gearbox loss function parameter c c_{gb}	0.0049		
Sea state		**condition**	
wave amplitude			
wave radial freq			
wave number k			
water depth at p			
standard gravity			

Headings
Purpose: To segment and provide focus for detailed information
Font size: 10 pt
Style: Concise and all sections should be numbered
First level heading: Bold
Second level heading: Italics and bold
Third level heading: Italics and not bold

4 Simulation experiments

This paper aims to investigate the behaviour of the propulsion plant in static conditions and during an acceleration manoeuvre under varying operational conditions with the simulation experiments described next.

4.1 Scenarios

The case study considered in this paper is a patrol vessel, similar to the RNLN *Holland* class, equipped with two medium speed diesel engines. The C4-40 propeller has been matched to the ship and diesel engine according to the procedure proposed in Klein Woud and Stapersma (2012), ensuring engine loading is within the continuous operating limit in the design condition, including the effect of waves. The resulting model parameters are listed in Table 3. The simulations are performed on a PC with Intel Core i5 processor and 8 GB memory in the MATLAB Simulink R2014b modelling environment.

4.1.1 Static working points in speed control regime

The first experiment investigates the behaviour of the propulsion plant in static working points, from 40% to 100%, in steps of 10%. The experiment is used to determine whether the engine is overloaded in static working points and to investigate the effect of the combinator curve on fuel consumption. The ship speed as a function of time during this manoeuvre is illustrated in Figure 8. The actual ship speed that is achieved during the progressive shaft speed settings depends on the specific conditions. We consider three situations:

- In the trial condition the ship is light loaded, the sea is considered flat and no fouling is assumed. This leads to a multiplication factor y of 0.75, because the resistance curve has been determined for design conditions.

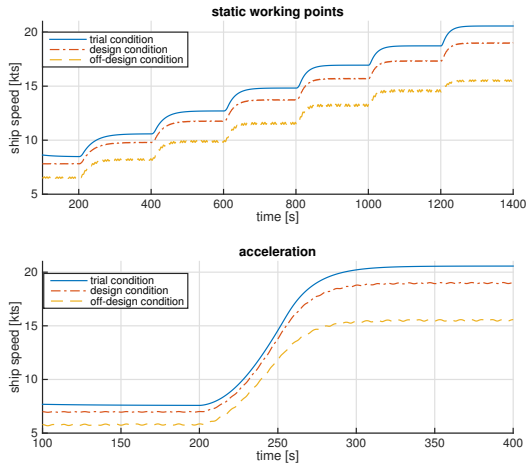

Figure 8: Ship speed for static points and during acceleration in speed control regime for trial, design and off-design conditions.

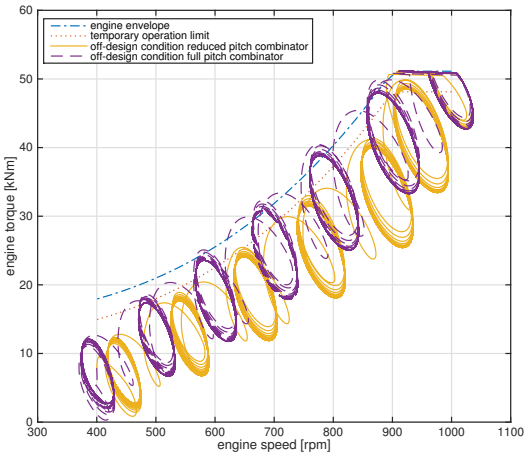

Figure 9: Engine speed and torque in static operating points with speed control for off-design condition with reduced and full pitch.

- In the design condition, the ship is loaded in design condition and average fouling and medium wind speed are considered. The multiplication factor y is 1 as the design resistance $R_{v_{max}}$ is taken under these conditions. Sea state 4 is represented by a wave amplitude ζ of 2 m (Gerritsma, 1989).
- In the off-design condition, the ship is heavily loaded, average fouling and high wind speed are considered and sea state is considered to be 7. This is represented by a multiplication factor y of 1.75 and a typical wave amplitude ζ of 5 m (Gerritsma, 1989).

The parameters used to represent the design and off-design conditions are listed in Table 3.

4.1.2 Acceleration in speed control regime

The second experiment investigates the behaviour of the propulsion plant during an acceleration in the speed control regime from a setting of 36% to 100%. The experiment is used to investigate the impact of torque control and alternative pitch schedules during acceleration on engine overloading, thermal loading, acceleration and propeller inflow angle, which is a measure for the probability of cavitation occurring (Vrijdag, 2009). The ship speed as a function of time during this manoeuvre is illustrated in Figure 8. The actual ship speed after acceleration depends on the conditions as outlined in the previous section4.1.1.

4.2 Results

4.2.1 Static working point using speed control and alternative combinator curves

First, the results in Figure 9 show that the reduced pitch combinator curve is required to prevent overloading, because with full pitch the engine loading in off-design condition exceeds the engine operating envelop. The maximum engine speed setting should be avoided in these extreme conditions, as the engine then runs at its limit continuously with waves causing engine speed to drop. Furthermore, the arrows in Figure 10 indicate how the operating point moves when changing from the reduced pitch to the full pitch combinator curve. In trial conditions the operating points remain well clear of the engine envelope limits.

Secondly, the results in Figure 11 show that the fuel consumption of the propulsion plant can be reduced by 1 to 3% by running the propulsion plant with the full pitch combinator curve in trial and design conditions, as the propeller open water efficiency then improves 1 to 3 %. An adaptive controller could increase pitch to improve efficiency when conditions allow this and reduce pitch when high load causes overloading. Furthermore, these results illustrate how important matching the engine for design conditions is, as an engine with too little power would overload in design conditions.

Moreover, note that the fluctuation of engine torque in the experiment is approximately 25% of nominal torque, where the significant fluctuation in the measurements presented in Figure 1, from van Spronsen and Toussain (2001), is

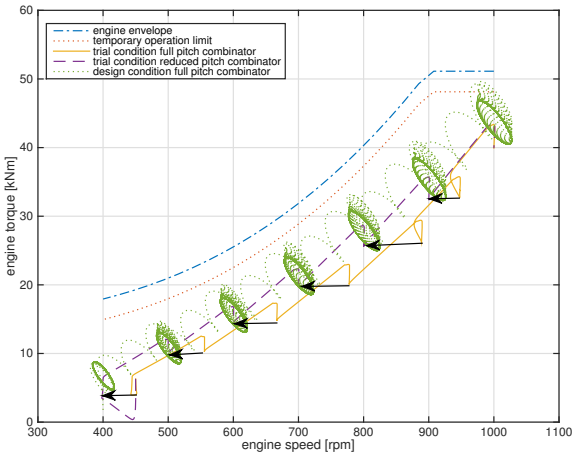

Figure 10: Engine speed and torque in phase plane in static operating points with speed control for trial condition with reduced and full pitch and for design condition with full pitch.

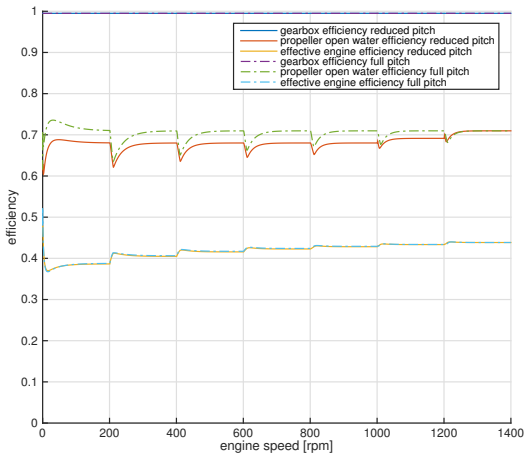

Figure 11: Gearbox, propeller and engine efficiencies in static operating points for trial condition with full pitch and reduced pitch combinator curves.

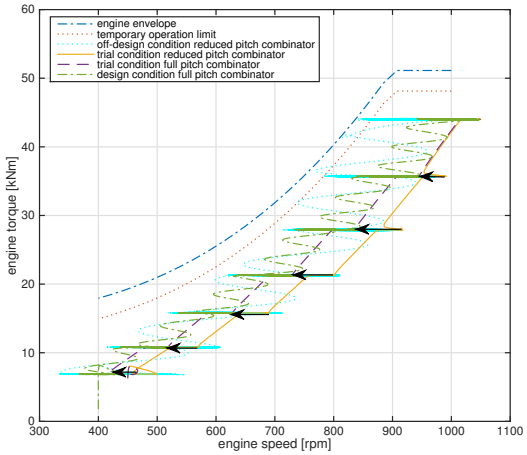

Figure 12: Engine speed and torque in phase plane in static operating points with torque control for trial, design and off-design condition with reduced pitch.

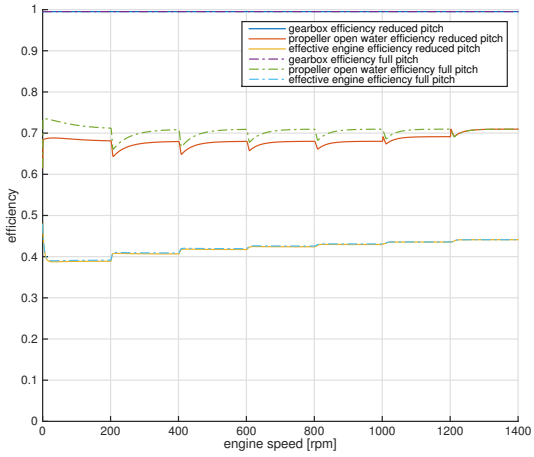

Figure 13: Gearbox, propeller and engine efficiencies in static operating points for trial condition with full pitch and reduced pitch combinator curves.

25% of nominal fuel rack position. More importantly, the orientation of the disturbance in the phase plane is similar to the measurements, even though the amplitude in the measurements is irregular. The regular behaviour in the simulation is due to simplifying the wave motion to a fixed frequency and amplitude as opposed to an irregular stochastic spectrum of real waves as measured and modelled in Aalbers and van Gent (1984).

4.2.2 Static working points using torque control

The results in Figure 12 show how torque control eliminates torque fluctuation at the expense of increased speed fluctuation. Interestingly the margin to the temporary operating limit and the engine envelope remains of similar magnitude. Therefore, in off-design condition pitch reduction is still required, Furthermore, Figure 13 shows fuel consumption can be reduced at trial condition by using the full pitch combinator curve, as with speed control. Moreover, the operating points with torque control, shown in Figure 12, move, as in Figure 10.

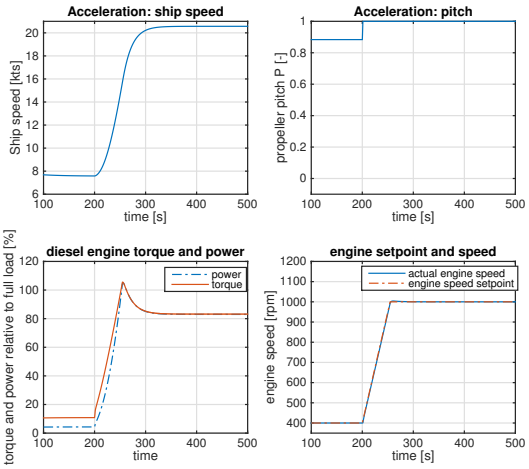

Figure 14: Acceleration with speed control in trial condition.

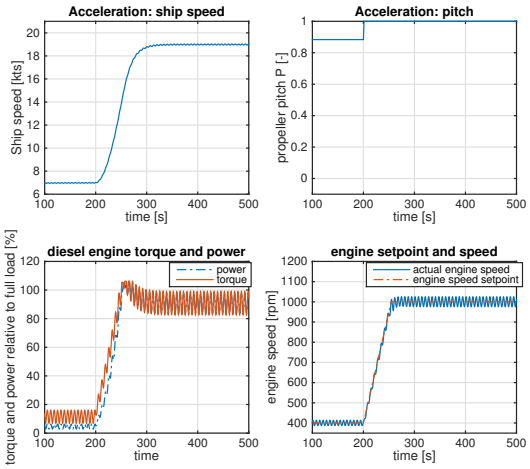

Figure 15: Acceleration with speed control in design condition.

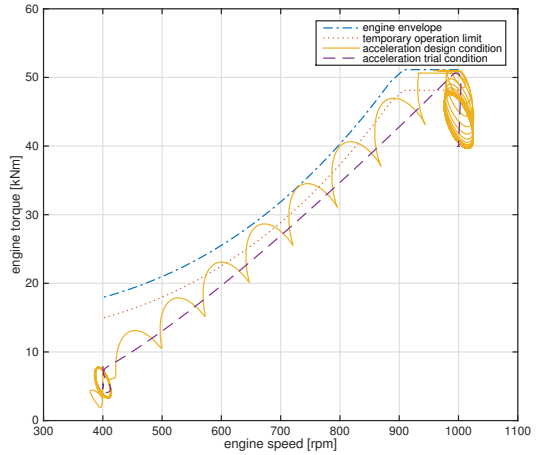

Figure 16: Engine speed and torque in phase plane during acceleration with speed control in trial and design conditions.

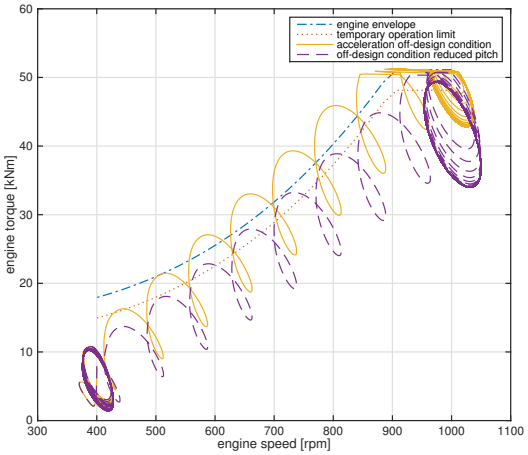

Figure 17: Engine speed and torque in during acceleration with speed control at full and reduced pitch in off-design condition.

4.2.3 Acceleration with speed control under various conditions

The behaviour of the system with conventional speed control during the acceleration manoeuvre is presented in Figures 14, 15 and 16 for trial and design conditions. Because the combinator curve for the new setting requires full pitch, the acceleration manoeuvre in the phase plane for the trial condition is already close to the temporary operating limit. During design conditions the engine is only slightly overloaded, because in the matching procedure an engine margin of 15% has been accounted for and because the shaft speed acceleration rate has been limited sufficiently. In other words, the shaft speed acceleration rate determines the angle at which the torque increases with increasing speed during the manoeuvre. This angle should not intersect the overload line. Under off-design conditions overloading does occur, as shown in Figure 17. This can be prevented by reducing pitch. This pitch reduction only has to be small, in this case 10% and can be kept constant during the manoeuvre. Fast and large pitch reduction, as reported in Vrijdag (2009) is not necessary.

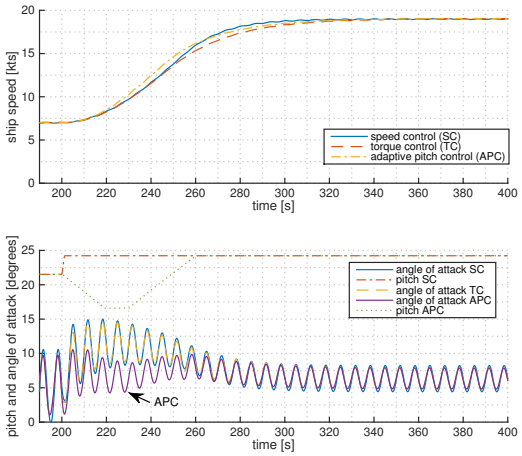

Figure 18: Propeller pitch and inflow angle during acceleration comparing comparing torque, speed and adaptive pitch control in design condition.

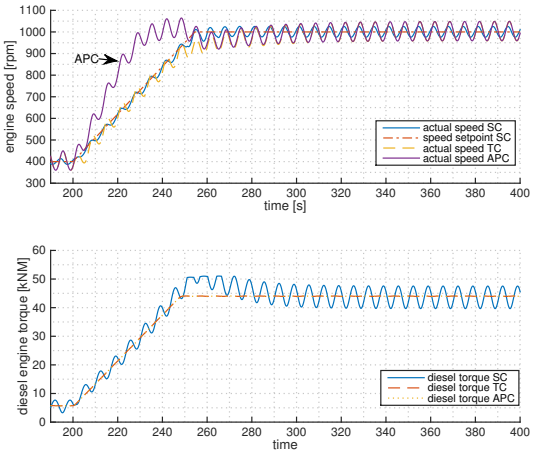

Figure 19: Engine speed and engine torque during acceleration comparing torque, speed and adaptive pitch control in design condition.

4.2.4 Acceleration with torque control under design conditions

The results in Figures 18, 19, 20 and 21 illustrate that torque control eliminates fluctuations in torque and thermal loading. The reduction in maximum cilinder temperature during the acceleration manoeuvre is 100K or 4%. During the acceleration the operating conditions cross the temporary operation limit less frequently and less seriously. At full torque, the torque does not risk crossing the temporary operation limit and the engine margin could potentially be used to increase ship speed, without the risk of overloading the engine.

On the contrary, speed fluctuation increases by 65% at maximum load. Furthermore, the strategy to maintain the maximum torque setting for every condition can lead to overspeed, although this could simply be prevented by including a minimum and maximum engine speed governor. Furthermore, with speed control, acceleration is faster when approaching stationary speed, because the shaft speed directly progresses to its stationary shaft speed. While the ship speed is still lower this leads to a higher torque loading coefficient and thus torque, as the hydrodynamic pitch angle is proportional to ship speed. With torque control, torque progresses to its final setpoint, so it takes longer to reach torque balance and thus the final ship speed.

4.2.5 Acceleration with torque control and reduced pitch during acceleration in design conditions

Figures 18, 19, 20 and 21 demonstrate three potential effects of an advanced pitch control strategy that reduces pitch during acceleration. First, the engine speed increases more quickly due to the reduced pitch, leading to a higher air excess ratio and 300 K, or 12% lower peak temperature during the acceleration. Secondly, the reduced pitch during acceleration leads to a maximum angle of attack onto the propeller of 10 degrees, also limiting cavitation noise (Vrijdag, 2009). Finally, engine power increases more quickly, due to the faster increase in engine speed, leading to faster acceleration.

5 Conclusions and further research

In conclusion, this paper has proposed torque control and an adaptive pitch control strategy to improve performance of direct drive diesel engine propulsion. Moreover, the paper presented a simulation strategy to investigate system performance. This simulation strategy included a wave model that represents waves as a single frequency and to include an irregular stochastic wave model and relate this model to actual sea states already gives a good indication of system behaviour, particularly when varying trim and loading conditions.

Conclusion
Purpose: Summarise the paper and include recommendations

The simulation experiments have shown that torque control can reduce thermal loading of diesel engines in moderate sea states by 4%. Furthermore, combining torque control with adaptive pitch control can improve acceleration performance, while further reducing thermal loading with an additional 8% and reducing cavitation noise during the

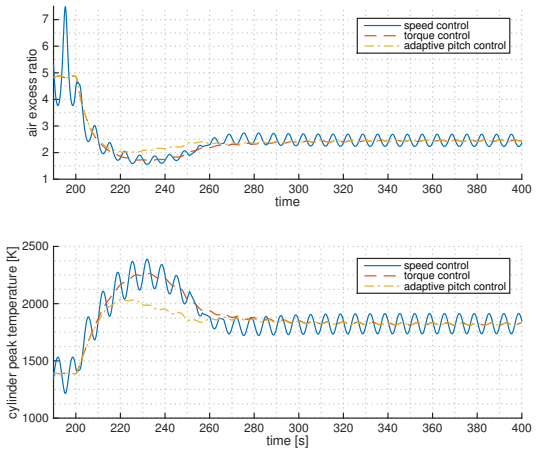

Figure 20: Air excess ratio and cylinder peak temperature during acceleration comparing torque, speed and adaptive pitch control in design condition.

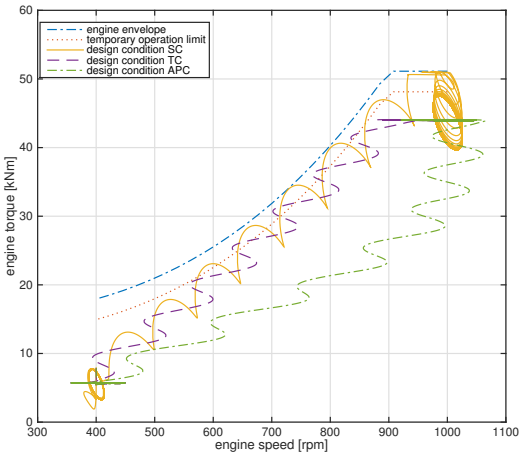

Figure 21: Engine torque and speed in phase plane during acceleration comparing torque, speed and adaptive pitch control in design condition.

acceleration. Moreover, adaptively changing pitch when sailing at constant speeds can improve fuel consumption by 1 to 3 %.

However, in the simulation study, the pitch settings were achieved with a schedule based control strategy. Furthermore, when applying torque control an additional speed controller to prevent under- and overspeed has to be integrated into the controller. Fu a controller that can actually maximise the improvements. This controller would timum pitch and torque trajectory in time for the trade-off between acceleration ding, cavitation noise and fuel consumption. With such a controller, direct drive tractive for naval mechanical and hybrid propulsion.

Acknowledgements
Purpose: To acknowledge individuals/ companies providing data/ information

Acknowledgement

This project is partially supported by the project "ShipDrive: A Novel Methodology for Integrated Modelling, Control, and Optimization of Hybrid Ship Systems" (project 13276) of the Dutch Technology Foundation STW and by the Royal Netherlands Navy. Figure 1, ©IFAC 2001, was reproduced from van Spronsen and Toussain (2001) with permission.

References

References
Purpose: To acknowledge referenced articles
Format: References should be listed in alphabetical order

Aalbers, A B., van Gent, W., 1984. Unsteady wake velocities due to waves and motions measured on a ship model in head wa In: Proceedings of the Fifteenth Symposium on Naval Hydrodynamics. Hamburg, Germany, pp. 69–81.

Betz, A., on rate and rate of heat release of turbocharged diesel engines under transien Zeitschrift. Vol. 47. Issue 7-8. pp. 263–267.

Blokland, iences and design consequences of integration in a naval vessel. In: Proceedi Conference. Bath, UK.

Dang, J., Brouwer, J., Bosman, R., Pouw, C., August 2012. Quasi-steady two-quadrant open water tests for the Wageningen Propeller C- and D-series. In: Proceedings of the Twenty-Ninth Symposium on Naval Hydrodynamics. Gothenburg, Sweden.

Dang, J., van den Boom, H., Ligtelijn, J. T., 2013. The Wageningen C- and D-series propellers. In: Proceedings of the 12th International Conference on Fast Sea Transportation. Amsterdam, the Netherlands.

de Waard, D. S., 2014. Parameterisation of ship propulsion drives. fuel efficiency under different operational modes and configurations. Msc. thesis, Faculty 3ME, Delft University of Technology, the Netherlands.

de Waard, D. S., 2015. Parameterization of ship propulsion drives and their fuel efficiency under different operatiobal modes and configurations. In: Proceedings of the Engine As A Weapon VI conference. Bath, UK, pp. 44–57.

Faber, E., 1993. Some thoughts in diesel marine engineering. In: SNAME Transactions. Vol. 101. pp. 537–582.

Gawn, R. W. L., 1952. Effect of pitch and blade width on propeller performance. In: Transactions of the Royal Institute of Naval Architecture. pp. 157–193.
Gerritsma, J., 1989. Bewegingen en sturen 1 - Golven. MT513, report 473-K. Delft University of Technology, Faculty 3ME.
Gerritsma, J., Beukelman, W., 1972. Analysis of the resistance increase in waves of a fast cargo ship. In: International Shipbuilding Progress. Vol. 19 (217). pp. 285–293.
Godjevac, 2009. Wear and friction in a controllable pitch propeller. PhD thesis, Faculty Mechanical, Maritime and Materials Engineering, Delft University of Technology.
Godjevac, M., Drijver, J., de Vries, L., Stapersma, D., 2015. Evaluation of losses in maritime gearboxes. In: Proceedings of the Institution of Mechanical Engineers, part M: Journal of Engineering for the Maritime Environment. pp. 1–16.
Grimmelius, H. T., Stapersma, D., May 2001. The impact of propulsion plant control on diesel engine thermal loading. In: Proceedings of the 22nd CIMAC World Congress. Hamburg, Germany.
Guillemette, J. R., Bussières, P., 1997. Proposed optimal controller for the Canadian patrol frigate diesel propulsion system. In: Proceedings of the 11th Ship Control Symposium. Vol. 1. Southampton, UK, pp. 507–530.
Klein Woud, H., Stapersma, D., 2012. Design of Propulsion and Electric Power Generation Systems. IMarEST, London, UK.
Kuiper, G., May 1992. The Wageningen Propeller Series. publication 92-001. MARIN.
Kyrtatos, N. P., Koumbarelis, I., 1991. Performance prediction of next generation slow speed diesel engines during ship manoeuvres. In: Tranactions of The Institute of Marine Engineers. Vol. 106, Part 1. pp. 1–26.
Liu, S., Papanikolaou, A., 2016. Fast approach to the estimation of the added resistance of ships in head waves. In: Ocean Engineering. Vol. 112. pp. 211–225.
Lyster, C. G., Dawe, T., 2015. Matching the propulsion system to the mission to reduce maintenance cost for OPVs. In: Proceedings of the Engine As A Weapon VI conference. Bath, UK.
Miedema, S. A., Lu, Z., June 12-15 2002. The dynamic behaviour of a diesel engine. In: Proceedings of the WEDA XXII Technical Conference and 34th Texas A and M Dredging Seminar. Denver, Colorado, USA.
Schulten, P., 2005. The interaction between diesel engines, ship and propellers during manoeuvring. PhD thesis, Faculty Mechanical, Maritime and Materials Engineering, Delft University of Technology.
Shi, W., Grimmelius, H. T., Stapersma, D., 2010. Analysis of ship propulsion system behaviour and the impact on fuel consumption. In: International Shipbuilding Progress. Vol. 57. pp. 35–64.
Stapersma, D., January 2010. Diesel Engines - A Fundamental Approach to Performance Analysis, Turbocharging, Combustion, Emissions and Heat Transfer, 8th Edition. Vol. 2: Turbocharging, Part I: Diesel Engines A - Performance Analysis and Turbocharging. Netherlands Defence Acedemy.
Stapersma, D., Grimmelius, H. T., 2009. A fresh view on propulsion control II. In: Proceedings of the 14th International Ship Control Systems Symposium. Ottawa, Canada.
Stapersma, D., Schulten, P. J. M., Grimmelius, H. T., 2004. A fresh view on propulsion control. In: Proceedings of the 7th International Naval Engineering Conference. Amsterdam, The Netherlands, pp. 221–240.
T[illegible]ower of Ships: a Manual of Marine Propulsion. Press of Ransdell, Inc., Wash-
[illegible] Sprønsen, T., Toussaint, R., July 2001. An optimal control approach to preventing marine diesel engine overloading aboard *Karel Doorman* class frigates. In: Proceedings of the IFAC conference on Control Applications in Marine
[illegible] operational conditions. PhD thesis, Faculty Mechanical, Maritime and Materials Engineering, Delft University of Technology, The Netherlands.
[illegible] Ship Propulsion. Springer-Verlag, London, UK.

Bibliography
Purpose: To list material/sources not cited

Nomenclature
Purpose: Definition of all symbols and physical quantities

Glossary of terms
Purpose: To explain acronyms and abbreviations

Appendices
Purpose: To explain lengthy data which would not fit comfortably with the main text